Lifetime of adsorbate vibrations: The role of anharmonicity

J. C. Ariyasu and D. L. Mills
Department of Physics, University of California, Irvine, California 92717

Kathryn G. Lloyd and John C. Hemminger
Department of Chemistry, University of California, Irvine, California 92717
(Received 27 March 1984)

We discuss calculations of the anharmonic damping of adsorbate vibrations, with application to species (S, O, CO) adsorbed on the Ni(100) and the Ni(111) surfaces. If the frequency of vibration of the adsorbate lies below twice the maximum phonon frequency of the substrate, then energy conservation allows it to be damped by emitting two substrate phonons. Also, in some cases, the adsorbate vibration can decay to a final state with one substrate phonon and one mode localized on the adsorbate. For the above-cited examples, we explore the magnitude and temperature variation of the linewidth of adsorbate modes from this mechanism. Near room temperature, the calculated linewidths exhibit a linear variation with temperature. For the C—Ni stretching mode of top-bonded CO, our results are in accord with the data of Chiang, Tobin, Richards, and Thiel [Phys. Rev. Lett. **52**, 648 (1984)]. We also simulate inhomogeneous broadening produced by disorder by considering the eigenfrequencies of infrared-active modes from pairs or small clusters of adsorbates. We find this source of broadening comparable to that provided by anharmonicity.

I. INTRODUCTION

While the vibrational properties of crystal surfaces and adsorbate layers have been studied by theorists for quite a number of years,[1] we have had very little experimental data in hand which depends sensitively on the microscopic details of the surface environment. Various kinds of surface acoustic waves generated by mechanical transducers have wavelengths which are very long compared to the lattice constant, and thus average over the microscopic details, although their propagation characteristics are influenced measurably by monolayer quantities of adsorbate.[1] High-frequency internal modes of vibration of adsorbed molecules have been studied by infrared or electron-energy-loss spectroscopy;[2] the frequencies of such modes may be influenced by the adsorption process, but the inferences which may be drawn from the data are indirect.

The situation has changed dramatically quite recently, since both inelastic atom-surface scattering[3] and electron-energy-loss spectroscopy[4] have reached a level of sophistication which allows one to measure the dispersion curves of surface phonons throughout the two-dimensional Brillouin zone. As is well known from similar studies of the bulk-phonon dispersion curves of crystals, the dispersion curves contain detailed information on microscopic aspects of the surface region.

While our knowledge of surface-phonon dispersion curves of both clean and adsorbate-covered surfaces is evolving rapidly as a consequence of the activity just cited, we have only limited information concerning the intrinsic linewidths of such modes. For some time, information on the intrinsic width of the stretching vibration of CO has been available,[5] and infrared methods have been employed to study the intrinsic width of the perpendicular vibration of hydrogen on the W(100) surface[6] and of hydrogen on the Si(111) surface.[7] In all these cases, the frequency of the adsorbate mode is sufficiently high so that if anharmonicity is to limit the lifetime, then energy conservation requires several phonons in the final state. By analogy with the analysis of multiphonon decay processes in bulk crystals,[8] we may expect that this mechanism will prove an inefficient means of damping. For such high-frequency adsorbate modes on metals, the dynamic electric dipole moment of the vibrating adsorbate may excite particle-hole pairs. Estimates based on a very simple model of this mechanism[9] suggest that it can indeed provide an account of the magnitude of the measured linewidth.

More recently, Chiang and co-workers have measured the intrinsic linewidth of the C—Ni stretching vibration for CO adsorbed on the Ni(100) surface.[10] This is done through analysis of the frequency spectrum of thermal radiation emitted from the sample when it is placed in a cooled environment. The C—Ni stretching mode of adsorbed CO lies at 480 cm^{-1} for this surface; a frequency sufficiently low to allow two-phonon decay processes by energy conservation. Thus, anharmonicity may be expected to play a more substantial role here than for the high-frequency modes cited above. Furthermore, the vibrational modes of oxygen and sulfur adsorbed on Ni(100) and Ni(111) surfaces lie above the maximum substrate phonon frequency of 300 cm^{-1}, but below 600 cm^{-1},[11] so, here, two-phonon processes are also allowed. These modes have been recently studied by electron-energy-loss spectroscopy,[11] although it is our understanding that the linewidth present in the data is of instrumental rather than intrinsic origin. Nonetheless, it is also interesting to inquire into the magnitude and temperature variation of the two-phonon contribution to the linewidth of these modes.

This paper presents a theoretical analysis of the two-

phonon contribution to the linewidth of the high-frequency vibrations of an adsorbate which resides in the fourfold hollow site of the (100) surface of a fcc crystal, or in the threefold hollow site of the (111) surface of such a material. Explicit application is to the mode for which the adsorbate motion is normal to the surface; these are the modes explored in infrared or near-specular electron-energy-loss spectroscopy, and it is these experimental methods that are most likely to provide information on intrinsic linewidths in the near future. We also consider the case of the C—Ni stretching vibrations for CO top bonded to a Ni atom on the Ni(100) surface. It is clear from the above remarks that our interest centers on those species for which the normal-mode vibration frequency lies above the maximum phonon frequency of the substrate, but below twice this value; it is only in this range where the two-phonon process explored here conserves energy.

Metiu and co-workers[12] have also explored damping of vibrations of adsorbates by anharmonicity. These authors were interested in the 2000-cm^{-1} range (i.e., very-high-frequency) vibrational modes of light adsorbates on metals. Examination of the diagrams retained in their calculation show they also confine their attention to two-phonon processes; the damping is then produced by the fact that they assign a finite linewidth to the substrate phonons. The damping of the adsorbate mode is thus an off-resonant process in their model, and exists because the very-high-frequency tail of the (two-phonon) substrate-mode Green's function overlaps the frequency of the adsorbate mode. In essence, this may be shown to be equivalent to the description of damping by multiphonon processes, with coupling to the multiphonon manifold transmitted via two-phonon states. The adsorbate-mode linewidth is estimated to be in the range of 1 cm^{-1}, a surprisingly large value when compared to multiphonon decay rates well known in bulk solids.[8] These authors assume the substrate phonon damping rate which enters their theory is frequency independent all the way out to the 2000-cm^{-1} regime. The same assumption applied to the estimate of infrared absorption in the multiphonon regime overestimates the absorption constant by many orders of magnitude.[8] In fact, the damping parameter falls off exponentially as one moves beyond the two-phonon bands of the solid.[8] This behavior should be noted in quantitative estimates of damping by means of multiphonon processes.

Our view is that, for adsorbates on metals, anharmonic damping is likely to compete with the particle-hole mechanism primarily in the frequency regime outlined earlier, where two-phonon decays may proceed directly in a manner which conserves energy. Our aim is to provide estimates of the strength and temperature variation of this mechanism for the adsorbate-substrate combinations outlined earlier. We shall see there is a strong, nearly linear temperature variation of the anharmonic damping rate near room temperature. This should allow one to discriminate between the mechanism explored here and the nominally temperature-independent damping provided by coupling to particle-hole pairs.

To render the calculation of the anharmonic damping rate tractable, it is convenient to make certain approximations. First, we consider an isolated adatom on the surface. The vibrational modes of interest all lie far enough above the substrate phonon bands to ensure that the vibrational motion is well localized in the very near vicinity of the adsorbate. It is thus reasonable to proceed through use of a model Hamiltonian within which all pairwise interactions are harmonic, except those between the adsorbate atom and its nearest neighbors in the substrate.[13] In essence, these are the only bonds which are flexed when the adsorbate vibration is excited. We describe these bonds through use of a Morse potential, adjusted to reproduce the harmonic force constants employed in earlier analyses, along with binding energies calculated by Upton and Goddard.[14] We then have no adjustable parameters. Within this simple model, we may relate the anharmonic damping rate to certain local-phonon spectral-density functions which were the subject of earlier theoretical analyses.[15] Here we need a considerable number of these functions; as a consequence, we generate them by means of a cluster calculation discussed below. For top-bonded CO, we require a model somewhat more complex than that just described.

While we find the two-phonon damping to be significant for the examples that we consider, other sources of linewidth are possible. For a measurement of the intrinsic linewidth associated with an isolated adatom to be carried out, clearly one must work well below the coverage appropriate to a single monolayer. No measurement of an adsorbate-mode linewidth has been yet reported for such low coverages. In fact, there is likely to be appreciable disorder present on the surfaces explored so far. A pair or small cluster of adatoms will absorb radiation at a frequency which differs from that of an isolated adatom, so the presence of disorder is a source of inhomogeneous broadening. If the inhomogeneous linewidth (nominally temperature independent) is comparable to the intrinsic contribution from the two-phonon mechanism explored here, the strong temperature variation we calculate may be partially obscured in infrared-absorption data. We have explored such inhomogeneous broadening within the same model that we use to calculate the linewidth, and find its magnitude significant. We also summarize these calculations in the present paper.

We have published a brief summary of these calculations elsewhere.[16] Some of the information presented here differs from that discussed in our earlier note. There we reported that the linewidth we calculate for the C—Ni mode of top-bonded CO on Ni(110) is in good accord with the data of Chiang and co-workers. Here we present calculations of the temperature variation of the linewidth over a wide temperature range. We inadvertantly omitted one contribution to the linewidth for oxygen adsorbed onto the threefold hollow site of Ni(111), so the linewidth reported here is considerably larger than that given earlier. Finally, we have found a new contribution to the linewidth of oxygen on Ni(100) not considered earlier; our value of the room-temperature linewidth of the high-frequency oxygen perpendicular mode is now brought from 20 to 40 cm^{-1}, in very good quantitative accord with the value inferred indirectly from electron-energy-

loss spectra by Andersson, Karlsson, and Persson.[17]

The outline of this paper is as follows: In Sec. II we discuss the model and derive the formulas which are the basis of the calculation; in Sec. III we present calculations of the local-spectral-density functions by the cluster method, and compare them with earlier results, including inhomogeneous broadening with origin in pairs or small clusters of adsorbate on the surface.

II. DERIVATION OF THE ANHARMONIC DAMPING RATE

In this section we develop a theoretical description of the anharmonic contribution to the damping of adsorbate vibrational modes. For the reasons discussed in Sec. I, we restrict our attention to modes that lie between the maximum substrate phonon frequency, ω_M, and $2\omega_M$, so that the vibrational mode localized on the adsorbate may decay via energy-conserving two-phonon processes. We assume that there is an isolated adsorbate atom located on a high-symmetry site of an otherwise perfect-crystal surface, and that the adsorbate is coupled to its nearest-neighbor substrate atoms via nearest-neighbor, central-force interactions. We shall modify this model for top-bonded CO, as discussed shortly.

The basic geometry is illustrated in Fig. 1, where we show the adsorbate and one of its nearest-neighbor substrate atoms. Let $\vec{R}$ be the separation between the substrate and adsorbate atom, i.e., $\vec{R}=\vec{R}_s-\vec{R}_A$, and let $\Phi(R)$ be the nearest-neighbor pair potential. Then if $\vec{R}_0$ is the vector from the adsorbate to the substrate atom when both are in equilibrium, and $\vec{u}=\vec{u}_s-\vec{u}_A$ is the relative displacement of the pair from equilibrium, we may expand $\Phi(R)$ in powers of $\vec{u}$,

$$\Phi(R)=\Phi(R_0)+\tfrac{1}{2}\Phi''(R_0)(\hat{n}\cdot\vec{u}) \times\{(\hat{n}\cdot\vec{u})+R_0^{-1}[u^2-(\hat{n}\cdot\vec{U})^2]\} +\tfrac{1}{6}\Phi'''(R_0)(\hat{n}\cdot\vec{u})^3+\cdots . \tag{2.1}$$

We have assumed the first derivative of the pair potential $\Phi'(R_0)=0$, a condition required if the adsorbate site is an equilibrium site, and we write $\vec{R}_0=\hat{n}R_0$, with $\hat{n}$ a unit vector. Then $\Phi''(R_0)$ and $\Phi'''(R_0)$ are the second and third derivatives of the pair potential, respectively.

Within our model, there are three basic decay processes we may consider. The first is one in which the adsorbate local mode of frequency ω_0 decays into a pair of substrate phonons which we denote as s_1 and s_2. Then energy conservation demands that $\omega_0=\omega_{s_1}+\omega_{s_2}$, with $0\le\omega_{s_1}\le\omega_M$ and $0\le\omega_{s_2}\le\omega_M$. A description of such decay processes may be obtained by retaining terms proportional to $u_A u_s^2$ in Eq. (2.1), after writing $\vec{u}=\vec{u}_A-\vec{u}_s$. This is an approximation which assumes the high-frequency adsorbate vibrational mode has a displacement field localized on the adsorbate atom, with substrate atoms only weakly excited, and, conversely, the substrate phonons in the range $0\le\omega_{s_1}\le\omega_M$ excite the adsorbate weakly. In the examples that we consider, this assumption is well justified. There are two other decay channels that operate in some instances. In the cases we explore here [an adsorbate in the fourfold hollow site of a (100) surface or one in the threefold hollow site of a (111) surface], one has the adsorbate mode polarized normal to the surface, as well as two other modes which are parallel to the surface and degenerate for these high-symmetry sites.[18] We may refer to the frequencies of these modes as $\omega_0^{(\perp)}$ and $\omega_0^{(\parallel)}$, respectively. Then if we consider damping of the perpendicular mode, and if $\omega_0^{(\perp)}>\omega_0^{(\parallel)}$, we may have a two-phonon process in which the perpendicular mode decays into a parallel polarized adsorbate mode plus a substrate phonon. We then have $\omega_0^{(\perp)}=\omega_0^{(\parallel)}+\omega_{s_1}$. In the approximation above, a description of this second process is found in the terms proportional to $u_A^2 u_s$. Similarly, if $\omega_0^{(\parallel)}>\omega_0^{(\perp)}$, we have a third process, in which a substrate phonon may be absorbed, exciting the adsorbate in the process. Here the frequency ω_s of the substrate phonon equals $\omega_0^{(\parallel)}-\omega_0^{(\perp)}$. A description of this process is contained in these same terms. In Fig. 2 we provide an illustration of the initial and final states for each of these processes.

The first of the three processes described above requires that the frequency $\omega_0^{(\perp)}$ lies in the range $\omega_M\le\omega_0^{(\perp)}\le 2\omega_M$. It is important to note that no such constraint applies to the second and third processes just described. Here we require only $|\omega_0^{(\perp)}-\omega_0^{(\parallel)}|\le\omega_M$, so this process may allow anharmonic damping by two-phonon processes *even if the*

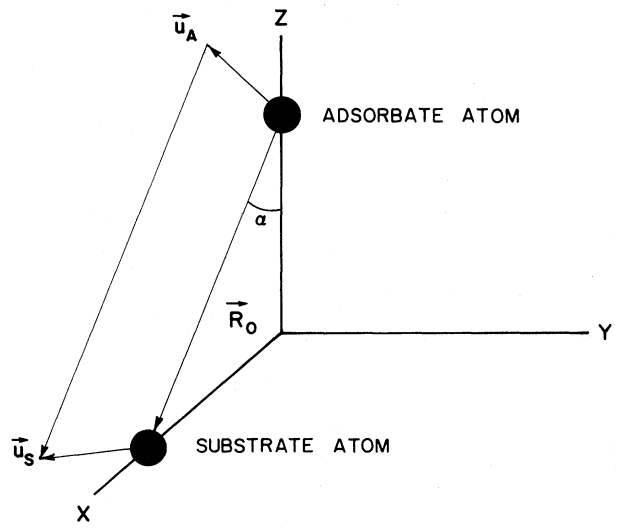

FIG. 1. Geometry employed in this calculation. The substrate lies in the half-space $z<0$, and the adsorbate sits a distance d above the surface. The vector $\vec{R}_0$ describes the equilibrium separation between the substrate and adsorbate, while α is the angle made by $\vec{R}_0$ and the vertical. Finally, $\vec{u}_s$ and $\vec{u}_A$ are the displacements of the substrate and adsorbate atoms from their respective equilibrium positions.

frequency of the mode in question is very large compared to ω_M. As we shall see, when they are allowed, the second and third processes may contribute importantly to the anharmonic damping rate. If we consider a polyatomic molecule adsorbed on the surface, if the separation between any two modes is less than ω_M, then each may have a lifetime limited by two-phonon processes, even though the frequency of each is large compared to ω_M. These remarks suggest that anharmonic damping by low-order processes may be of substantial importance in limiting the lifetime of even high-frequency adsorbate vibrations.

In an earlier paper, which presented a brief account of our results,[16] we found a very narrow linewidth for the case of oxygen on Ni(111), while Fig. 6 presented here gives a much more substantial value of 5.1 cm^{-1} at $T=300$ K. In the calculations reported earlier, we inadvertently omitted the contribution from the damping process which involves one substrate phonon and one transversely polarized adsorbate mode. Since the frequency of the perpendicular mode of oxygen on Ni(111) lies very close to $2\omega_M$, the two-phonon density of states at the perpendicular-mode frequency is very small. Thus, decay to one substrate phonon plus the transverse mode provides the dominant contribution to the linewidth.

If the terms just described are isolated in Eq. (2.1), then we have the piece $\tilde{\Phi}(R)$ of $\Phi(R)$ given by

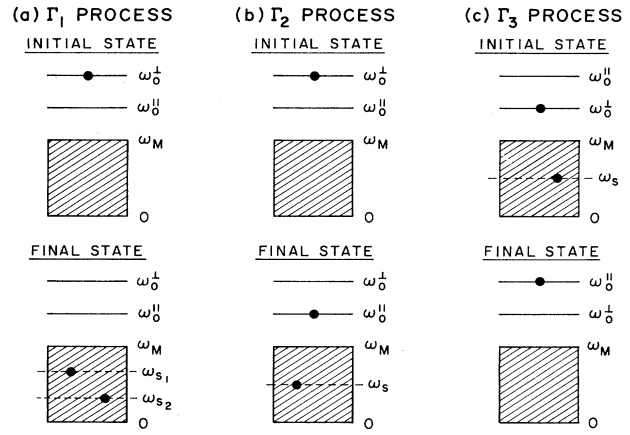

FIG. 2. Three processes which contribute to the two-phonon anharmonic linewidth. (a) The adsorbate mode, with frequency ω_0, can decay with emission of two substrate phonons ω_{s_1} and ω_{s_2}. This gives the contribution Γ_1 to the linewidth. (b) The adsorbate mode can decay to a substrate phonon ω_s, and a second localized parallel mode $\omega_0^{\parallel}$, if there is a local adsorbate parallel mode with frequency $\omega_0^{\parallel} < \omega_0^{\perp}$. This gives the contribution Γ_2 to the linewidth. (c) The adsorbate mode can also absorb a substrate phonon ω_s, to be excited to a parallel adsorbate mode with frequency $\omega_0^{\parallel} > \omega_0^{\perp}$. This is the process referred to in the text as Γ_3.

$$\tilde{\Phi}(R) = -V_2[u_s^2(\hat{n}\cdot\vec{u}_A)+2(\vec{u}_s\cdot\vec{u}_A)(\hat{n}\cdot\vec{u}_s)]-3\delta V(\hat{n}\cdot\vec{u}_s)^2(\hat{n}\cdot\vec{u}_A)$$
$$+V_2[u_A^2(\hat{n}\cdot\vec{u}_s)+2(\vec{u}_s\cdot\vec{u}_A)(\hat{n}\cdot\vec{u}_A)]+3\delta V(\hat{n}\cdot\vec{u}_s)(\hat{n}\cdot\vec{u}_A)^2 . \quad (2.2)$$

We have defined

$$V_2=(1/2R_0)\Phi''(R_0) , \quad (2.3a)$$

$$V_3=\tfrac{1}{6}\Phi'''(R_0) , \quad (2.3b)$$

and

$$\delta V=V_3-V_2 . \quad (2.3c)$$

If we assume that the adsorbate–substrate bond may be modeled by a Morse potential, it is possible to obtain simple expressions for V_2 and V_3. If $\omega_0^{(\perp)}$ is the frequency of the perpendicularly polarized adsorbate vibrational mode, we find that we may write

$$V_2=\frac{M_r(\omega_0^{(\perp)})^2}{2zR_0\cos^2\alpha} \quad (2.4a)$$

and

$$V_3=-\frac{1}{zD_e^{1/2}}\left[\frac{M_r(\omega_0^{(\perp)})^2}{2\cos^2\alpha}\right]^{3/2} . \quad (2.4b)$$

Here, z is the number of nearest-neighbor substrate atoms, the angle α is defined in Fig. 1, D_e is the dissociation energy, and

$$1/M_r=1/M_A+[1/(zM_s\cos^2\alpha)] ,$$

with M_A and M_s the masses of the adsorbate and substrate atoms, respectively. We have used an approximate expression for $\omega_0^{(\perp)}$ derived elsewhere to obtain this result.[16]

We ultimately want to express the anharmonic interaction in Eq. (2.2) in terms of the annihilation and creation operators of the phonon normal modes of the system. When the adatom is placed on the crystal surface, each normal mode is an admixture of adatom motion and motion of substrate atoms. There are two classes of normal modes: In a manner familiar from the lattice dynamics of infinite crystals with an impurity present, those which have a frequency above the maximum phonon frequency ω_M of the substrate have eigenvectors localized to the very near vicinity of the adsorbate. Assumptions outlined above presume that, to first approximation for the modes of interest in the present analysis, the small-amplitude motions of the substrate atoms play a minor role in modulating the bond distance between the adsorbate and its nearest neighbors on the substrate. The modes below ω_M are all necessarily spatially extended; if the crystal has a finite number N of atoms, then the motion of each atom, including the adsorbate, contributes a fraction proportional to $\hbar\omega/N$ to the total excitation energy $\hbar\omega$. The crystal with adsorbate present retains no translational symmetry, so the normal modes of the system do not have a well-defined wave vector. We consider the sample to have a finite number N of atoms, with $M_{\vec{l}}$ the mass of the atom at site $\vec{l}$, and denote the collection of quantum numbers used to describe a single mode by the symbol s. Then the displacement operator $\vec{u}(\vec{l})$ for the atom at site $\vec{l}$ may be written

$$\vec{u}(\vec{l})=\sum_s \left[\frac{\hbar}{2M_{\vec{l}}\omega_s}\right]^{1/2} \hat{e}_s(\vec{l})(a_s^\dagger+a_s) , \tag{2.5}$$

where ω_s is the frequency of mode s, a_s and $a_s^\dagger$ are the boson annihilation and creation operators, and $\hat{e}_s(\vec{l})$ is the eigenvector of the mode, normalized so that

$$\sum_{\vec{l}} |\hat{e}_s(\vec{l})|^2=1 . \tag{2.6}$$

When the form in Eq. (2.2) is combined with Eq. (2.5), and the total anharmonic potential is constructed by summing over all of the nearest neighbors to the adsorbate, we may write

$$\tilde{\Phi}_{\rm tot}=\tilde{\Phi}_1+\tilde{\Phi}_2 , \tag{2.7}$$

where $\tilde{\Phi}_1$ describes the decay of the local mode in question, here referred to by the operators a_0 and $a_0^\dagger$, into two substrate phonons, and $\tilde{\Phi}_2$ is the contribution from the process involving one localized phonon and one substrate mode. The first of these may be written in the form

$$\tilde{\Phi}_1=\sum_{s_1,s_2} \frac{M_1(s_1,s_2)}{(\omega_{s_1}\omega_{s_2})^{1/2}}(a_{s_1}^\dagger a_{s_2}^\dagger a_0+a_{s_1}a_{s_2}a_0^\dagger) , \tag{2.8}$$

where our prescription for constructing $M_1(s_1,s_2)$ has been given above. A similar form describes the second and third processes illustrated in Fig. 2, but in the interest of brevity, we omit explicit discussion of these.

To lowest order in the anharmonicity, it is a straightforward application of the golden rule to calculate the damping rate, Γ, of the local mode. We do this in the occupation-number representation. All normal modes $\{s\}$, of the system are in thermal equilibrium, except for the local mode itself. Thus, the occupation numbers of all modes except the local mode are given by the Bose-Einstein function

$$\bar{n}_s=[\exp(\hbar\omega_s/k_BT)-1]^{-1} ,$$

while the occupation number n_0 of the local mode differs from $\bar{n}_0$, the Bose-Einstein value. The golden rule then gives the decay rate

$$\frac{dn_0}{dt}=-\Gamma(n_0-\bar{n}_0) , \tag{2.9}$$

with

$$\Gamma=\Gamma_1+\Gamma_{2,3} \tag{2.10}$$

broken down into the two basic processes discussed above (for the systems considered here, the second and third processes cannot contribute to the damping rate simultaneously). We have

$$\Gamma_1=\frac{8\pi}{\hbar^2}\sum_{s_1,s_2} \frac{[1+\bar{n}(\omega_{s_1})+\bar{n}(\omega_{s_2})]}{\omega_{s_1}\omega_{s_2}} |M_1(s_1,s_2)|^2 \times\delta(\omega_0-\omega_{s_1}-\omega_{s_2}) , \tag{2.11}$$

and once again a similar expression applies for Γ_2 and Γ_3.

While this expression is simple in overall structure, its evaluation entails summing a rather complicated function over the normal modes of the substrate, as we shall see shortly. Many of the intermediate formulas are complex and of little general interest, but some remarks on their structure will prove useful. Quite clearly, if $\vec{e}_s(\vec{\delta})$ is the eigenvector associated with mode s for the nearest neighbor to the adsorbate at the site $\vec{\delta}$, then $M_1(s_1,s_2)$ has the general structure

$$M_1(s_1,s_2)=\sum_{\mu,\nu}\sum_{\vec{\delta}} f_{\mu\nu}^{(1)}(\vec{\delta})e_\mu^{s_1}(\vec{\delta})e_\nu^{s_2}(\vec{\delta}) . \tag{2.12}$$

A similar expression may be used to generate the matrix elements for the second and third processes, but on the right-hand side we have the combination $e_\mu^{s_1}(\vec{\delta})e_\nu^{s_2}(A)$, with s_2 the localized mode involved in the decay, and $e_\nu^{s_2}(A)$ the eigenvector which describes the adsorbate motion when the high-frequency parallel polarized local mode is excited.

It is convenient to introduce certain phonon spectral-density functions similar to those studied elsewhere:[15]

$$\rho_{\mu\nu}(\vec{\delta},\vec{\delta}';\omega)=\sum_s e_\mu^s(\vec{\delta})e_\nu^s(\vec{\delta}')\delta(\omega-\omega_s) . \tag{2.13}$$

Then, if z is the number of nearest neighbors to which the adsorbate is bonded and $\vec{\delta}_0$ is a particular neighbor chosen as a fiducial site, we may write, for the decay rate Γ_1,

$$\Gamma_1=\frac{8\pi z}{\hbar^2}\sum_{\substack{\kappa,\lambda\\ \mu,\nu}}\sum_{\vec{\delta}} f_{\mu\nu}^{(1)}(\vec{\delta}_0)f_{\kappa\lambda}^{(1)}(\vec{\delta}) \times\int_0^{\omega_M}\frac{d\omega}{\omega(\omega_0-\omega)}[1+\bar{n}(\omega)+\bar{n}(\omega_0-\omega)] \times\rho_{\mu\kappa}(\vec{\delta}_0,\vec{\delta};\omega)\rho_{\nu\lambda}(\vec{\delta}_0,\vec{\delta};\omega_0-\omega) , \tag{2.14}$$

where the right-hand side is independent of which neighbor is chosen as the reference site. Similar expressions may be derived for Γ_2 and Γ_3, but, again, in the interest of brevity, we do not give their explicit form.

For a given choice of adsorbate site, many terms contribute to the right-hand side of Eq. (2.14). Their number may be reduced through exploitation of symmetry, but the final total remains substantial. As an example, we consider an adsorbate which resides in a threefold hollow site. If we replace $\vec{\delta}_0$ by the symbol 1, and refer to a selected nearest neighbor to the fiducial site by the symbol 2 (if site 1 is located on the x axis, then site 2 is that obtained by a 120° counterclockwise rotation obtained by looking down on the crystal), then Γ_1 may be written in terms of $\rho_{\mu\nu}(1,1;\omega)$, and $\rho_{\mu\nu}(1,2;\omega)$. Six combinations of anharmonic coupling constants introduced earlier enter the final expression. These are

$$v_1=(V_2+3\,\delta V\sin^2\alpha)\cos\alpha , \tag{2.15a}$$

$$v_2=V_2\cos\alpha , \tag{2.15b}$$

$$v_3=3(V_2+3\,\delta V\cos^2\alpha)\cos\alpha , \tag{2.15c}$$

$$v_4=(V_2+3\,\delta V\cos^2\alpha)\sin\alpha , \tag{2.15d}$$

$$v_5=(V_2+\tfrac{3}{4}\,\delta V\sin^2\alpha)\cos\alpha , \tag{2.15e}$$

$$v_6=(V_2+\tfrac{9}{4}\,\delta V\sin^2\alpha)\cos\alpha . \tag{2.15f}$$

Then we have

$$\Gamma_1=\frac{3\pi\hbar}{M_s^2M_A\omega_0}\int_0^{\omega_M}\frac{d\omega[1+\bar{n}(\omega)+\bar{n}(\omega_0-\omega)]}{\omega(\omega_0-\omega)}$$

$$\times[\,v_1^2\rho_{xx}(1,1;\omega)\rho_{xx}(1,1;\omega_0-\omega)+2v_1v_3\rho_{xz}(1,1;\omega)\rho_{xz}(1,1;\omega_0-\omega)$$

$$+v_2^2\rho_{yy}(1,1;\omega)\rho_{yy}(1,1;\omega_0-\omega)+v_3^2\rho_{zz}(1,1;\omega)\rho_{zz}(1,1;\omega_0-\omega)$$

$$-4v_1v_4\rho_{xx}(1,1;\omega)\rho_{xz}(1,1;\omega_0-\omega)+4v_4^2\rho_{xx}(1,1;\omega)\rho_{zz}(1,1;\omega_0-\omega)$$

$$-4v_3v_4\rho_{zz}(1,1;\omega)\rho_{xz}(1,1;\omega_0-\omega)+2v_5(v_2+3v_2)\rho_{xx}(1,2;\omega)\rho_{xx}(1,2;\omega_0-\omega)$$

$$+2(v_1v_6+v_2v_5)\rho_{xy}(1,2;\omega)\rho_{xy}(1,2;\omega_0-\omega)+2v_2(3v_5+v_6)\rho_{yy}(1,2;\omega)\rho_{yy}(1,2;\omega_0-\omega)$$

$$+\tfrac{1}{2}v_3(4v_1-\sqrt{3}v_5+3v_6)\rho_{xz}(1,2;\omega)\rho_{xz}(1,2;\omega_0-\omega)$$

$$+\tfrac{1}{2}v_3(4v_1+\sqrt{3}v_5+v_6)\rho_{yz}(1,2;\omega)\rho_{yz}(1,2;\omega_0-\omega)+2v_3^2\rho_{zz}(1,2;\omega)\rho_{zz}(1,2;\omega_0-\omega)$$

$$+4\sqrt{3}v_2v_5\rho_{xx}(1,2;\omega)\rho_{xy}(1,2;\omega_0-\omega)+2v_4(v_1+v_5)\rho_{xx}(1,2;\omega)\rho_{xz}(1,2;\omega_0-\omega)$$

$$-12v_2v_5\rho_{xx},(1,2;\omega)\rho_{yy}(1,2;\omega_0-\omega)-2\sqrt{3}v_4(v_2+v_5)\rho_{xx}(1,2;\omega)\rho_{yz}(1,2;\omega_0-\omega)$$

$$-4v_4^2\rho_{xx}(1,2;\omega)\rho_{zz}(1,2;\omega_0-\omega)-2\sqrt{3}v_4v_6\rho_{xy}(1,2;\omega)\rho_{xz}(1,2;\omega_0-\omega)$$

$$-2v_4(v_2+v_6)\rho_{xy}(1,2;\omega)\rho_{yz}(1,2;\omega_0-\omega)+v_3(\sqrt{3}v_6-v_5)\rho_{xz}(1,2;\omega)\rho_{yz}(1,2;\omega_0-\omega)$$

$$-4\sqrt{3}v_2v_5\rho_{yy}(1,2;\omega)\rho_{xy}(1,2;\omega_0-\omega)+2\sqrt{3}v_2v_4\rho_{yy}(1,2;\omega)\rho_{yz}(1,2;\omega_0-\omega)$$

$$-5v_3v_4\rho_{zz}(1,2;\omega)\rho_{xz}(1,2;\omega_0-\omega)+\sqrt{3}v_3v_4\rho_{zz}(1,2;\omega)\rho_{yz}(1,2;\omega_0-\omega)]\,. \tag{2.16}$$

We have also derived an expression for Γ_1 for the case where the adsorbate resides in the fourfold hollow site; the final expression is actually lengthier than that in Eq. (2.16). Also, we have explicit forms for Γ_2 and Γ_3 for these two sites.

The continued-fraction method has been used in earlier work[15] to generate phonon spectral-density functions such as those which appear in Eq. (2.16). The method converges rapidly, but involves an extrapolation procedure which must be performed for each spectral-density function calculated. When one considers the total number of spectral densities required to evaluate Γ_1 and Γ_2 for the adsorbate/substrate geometries of interest here, a very large expenditure of labor is required to generate all the required functions.

Since all of the spectral-density functions that we require describe the *local* response of the substrate to vibrational motion of the adsorbate, one may generate the required spectral densities through the use of a finite cluster of atoms, provided the cluster is sufficiently large such that edge effects do not greatly influence the response of the adsorbate and its nearest neighbors. One thus proceeds as follows: Consider a substrate which contains N atoms with an adsorbate present. All of the vibrational frequencies and all of the eigenvectors may be generated by diagonalizing a $3(N+1)\times3(N+1)$ matrix. Without further need to diagonalize a large matrix, through direct use of the definition in Eq. (2.13) one may generate all of the required spectral-density functions. The results are smoothed by replacing the Dirac δ functions by appropriately normalized Lorentzians. We describe the details of the method in Sec. III, where selected results generated by this procedure are shown to agree well with fully converged continued-fraction calculations.

III. APPROXIMATE CALCULATIONS OF THE SPECTRAL DENSITIES

As we have seen, the evaluation of the large number of local spectral densities which we require is a formidable task. With the adsorbate in place, translational symmetry is completely broken, so we cannot exploit Bloch's theorem in the two directions parallel to the surface in order to construct the phonon eigenvectors. Earlier work[15] has shown that the continued-fraction method works very well for problems such as the one addressed here, but the method will prove very tedious if we wish to generate the large number of spectral densities needed.

Instead, we have used a cluster method to generate the required functions. We choose a finite number of metal atoms to mimic the substrate, and place an adsorbate in an appropriate surface site. Then we find the eigenfrequencies and eigenvectors of all of the vibrational modes of the cluster. The spectral-density functions are then calculated through direct resort to Eq. (2.13), with the Dirac δ functions replaced by suitably normalized Lorentzians. If the width of the Lorentzian is chosen to be 2 or 3 times the average spacing between the normal modes of the cluster, we obtain a smooth function that closely follows the results of fully converged continued-fraction calculations. The metal cluster is chosen to be sufficiently large so that end effects have little influence on the vibrational motion of the adsorbate and its nearest neighbors. In practice, one requires about 95 substrate atoms to achieve this limit. The size of the matrix that needs to be diagonalized is then $3N\times 3N$, where N is the total number of atoms in the cluster. This requires us to diagonalize a rather large matrix, but for a given choice of force constants or geometry, this need be done only once, and one may synthesize as many spectral-density functions as one wishes.

Our calculations utilize the F-G matrix method developed by Wilson.[19] This is a well-established technique in the field of molecular vibration theory.[20] Of course, the harmonic approximation was used to generate the spectral densities. For convenience, we express the vibrational potential energy in terms of internal (valence) coordinates such as bond-stretching coordinates, angle-bending coordinates, etc.[19] Perhaps a brief sketch of the method will prove helpful for the reader unfamiliar with it.

The potential energy in the harmonic approximation is written in the form

$$V=\tfrac{1}{2}\sum_{i,j} f_{ij}S_iS_j=\tfrac{1}{2}\vec{S}^{\,\dagger}\underline{F}\vec{S}\ , \tag{3.1}$$

where $\vec{S}$ is a vector formed from the set of internal coordinates, and the matrix $\underline{F}$ is constructed from the force constants:

$$f_{ij}=\left[\frac{\partial^2 V}{\partial S_i\,\partial S_j}\right]_0 . \tag{3.2}$$

The $\vec{S}$ vector is related to the Cartesian components of displacement $\{\vec{u}(\vec{l})\}$ by a transformation matrix $\underline{B}$:

$$\vec{S}=\underline{B}\,\vec{u}\ . \tag{3.3}$$

For convenience, as in solid-state lattice dynamics, one works with mass-weighted coordinates,

$$\vec{q}(\vec{l})=(\overline{M}_{\vec{l}})^{1/2}\vec{u}(\vec{l})\ , \tag{3.4}$$

so that

$$\vec{S}=\underline{B}\,\underline{M}^{-1/2}\vec{q}\equiv\underline{D}\,\underline{q}\ , \tag{3.5}$$

in matrix notation. Here $\underline{M}^{-1/2}$ is a diagonal matrix formed in the appropriate manner from the atomic masses.

Within this notation, the vibrational kinetic energy becomes

$$T=\tfrac{1}{2}\vec{P}^{\,\dagger}(\underline{D}\,\underline{D}^{\dagger})\vec{P}\ , \tag{3.6}$$

where $\vec{P}$ is a vector formed from momenta conjugate to the internal coordinates $\vec{S}$. One is then led to a secular equation of the form

$$|\,\underline{D}^{\dagger}\underline{F}\,\underline{D}-\omega^2\underline{I}\,|=0\ , \tag{3.7}$$

where the collection of eigenvalues $\{\omega_s^2\}$ of the $3N\times 3N$ matrix $\underline{D}^{\dagger}\underline{F}\,\underline{D}$ are the set of normal-mode eigenfrequencies of the cluster. The eigenvectors of the matrix $\{\underline{D}^{\dagger}\underline{F}\,\underline{D}\}$ are those which appear in the definition of the spectral densities in Eq. (2.13).

As remarked earlier, the spectral densities are calculated by replacing the Dirac δ functions in Eq. (2.13) by suitable Lorentzians. We then have

$$\rho_{\mu\nu}(\vec{\delta},\vec{\delta}';\omega)=\frac{1}{\pi}\sum_s e_\mu^s(\vec{\delta})e_\nu^s(\vec{\delta}')\frac{\gamma}{(\omega-\omega_s)^2+\gamma^2}\ . \tag{3.8}$$

There is a sum rule which requires that the integral of $\rho_{\mu\nu}(\vec{\delta},\vec{\delta}';\omega)$ over all frequencies equal unity when $\mu=\nu$ and $\vec{\delta}=\vec{\delta}'$, and be zero otherwise. Note that this property is preserved by the approximate form in Eq. (3.8).

As is the case for the continued-fraction approach,[15] the present method fails to provide an adequate representation of the spectral densities in the low-frequency regime, where long-wavelength acoustical phonons dominate. In essence, for frequencies so low that the phonon wavelengths are comparable to or larger than the cluster size, we obtain a poor representation of the spectral-density functions. The continued-fraction method breaks down at low frequencies for a very similar reason; in the approach, one samples only a finite number of atoms in the near vicinity of the site of interest, with the consequence that one obtains a poor account of the role of low-frequency, long-wavelength phonons. One may show that as $\omega\to 0$, the local-phonon density of states must vanish as ω^2. We force this frequency dependence on the spectral densities by matching an ω^2 law to their amplitude at 60 cm^{-1}. We have checked that the calculations of the anharmonic damping described in this paper are very insensitive to the details of this low-frequency extrapolation procedure.

In all of the calculations, we have used the nearest-neighbor bond-stretching model used in earlier work.[18] This model provides quite a good description of the bulk

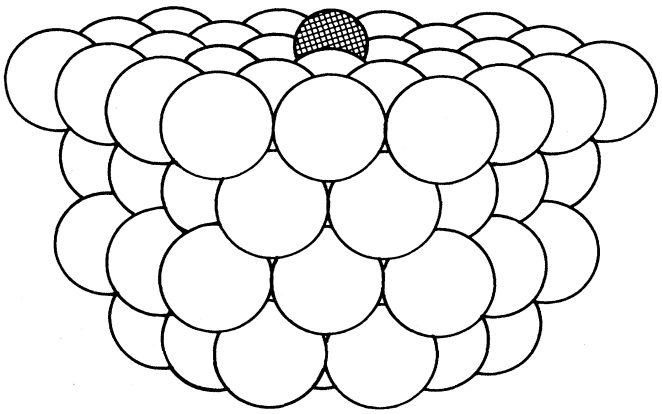

FIG. 3. The 76-atom cluster used to generate the spectral densities for adsorbates on the Ni(111) surface. The open spheres are the substrate atoms, and the shaded sphere is an adsorbate bounded to the threefold hollow site.

nickel phonon spectrum, as well as the influence of adsorbates on the vibration spectrum.

Both the size and the shapes of the nickel clusters have been chosen to optimize the agreement between the spectral densities that we calculate for a clean Ni surface and those calculated by Black using the continued-fraction method.[21] The cluster used for the Ni(111) calculations (see Fig. 3) contains 76 Ni atoms arranged in four layers. In Fig. 4 we compare our calculations of $\rho_{zz}(\omega)$ (the spectral density associated with the autocorrelation function which describes vertical motion of a Ni atom in the surface layer) with the earlier calculations of Black for an atom in the bare Ni(111) surface, and for an atom in the Ni(111) surface layer that is one of the three nearest neighbors to the adsorbate. The Ni—O stretching force constant was taken from the work of Upton and Goddard[14] and is given in Table I.

In Fig. 4 we compare the results of our cluster calculation with the fully converged continued-fraction calculations reported by Black.[21] In Fig. 4(a) we present his calculation of $\rho_{zz}(\omega)$, the spectral density which describes the frequency spectrum of vertical motion of an atom on the Ni(111) surface. In Fig. 4(b) we present our cluster results. The principal feature near 120 cm^{-1} in Black's result is reproduced nicely, and the overall shape of the spectral density is given properly by our method. We have compared selected examples of our other spectral densities with Black's results in order to find comparable agreement. We believe that the cluster results are accurate enough that quantities such as our damping rate, which depend on integrals of slowly varying functions with the spectral density, may be calculated accurately with them.

In Fig. 5 we show our cluster results for the spectral densities which describe perpendicular and parallel motion of oxygen on the Ni(111) surface [Fig. 5(a)] and on the Ni(100) surface [Fig. 5(b)]. One may appreciate that, in both cases, virtually all the spectral weight is concentrated in the strong peak centered around the high-frequency mode, very nearly localized on the adsorbate. Similarily, when the spectral density of substrate atoms which are nearest neighbors to the adsorbate are considered, nearly all the integrated strength is stored in the frequency regime between 0 and ω_M, the maximum substrate phonon frequency. These two observations are the motivation for the simplified forms utilized in the model of anharmonic coupling between the adsorbate and substrate discussed in Sec. II. Note that for oxygen on Ni(100), the parallel mode of the adsorbate lies *above* the perpendicular mode in frequency. Thus, here the contri-

TABLE I. Values of the force constants used in the various calculations described in the text. The bond-stretching force constants, denoted by the symbol k with suitable subscripts, are in units of mdyn/Å, while the units of the angle-bending force constants ρ are mdynÅ/rad^2. Finally, the adsorbate-substrate distance assumed is tabulated in angstroms.

O/Ni(100)[a]	S/Ni(100)[a]	O/Ni(111)[a]	S/Ni(111)[a]
$k_{Ni-O}=1.6296$	$k_{Ni-S}=1.2670$	$k_{Ni-O}=2.0775$	$k_{Ni-S}=1.8440$
$R_\perp=0.88$	$R_\perp=1.24$	$R_\perp=1.179$	$R_\perp=1.489$
	CO/Ni(100)		
	Force field 1[b]	Force field 2[c]	
	$k_{Ni-C}=1.8567$	$k_{Ni-C}=2.600$	
	$k_{C-O}=17.716$	$k_{C-O}=16.800$	
	$\rho_{Ni-C-O}=0.2981$	$\rho_{Ni-C-O}=0.380$	
	$R_{Ni-C}=1.94$	$\rho_{Ni-Ni-C}=0.230$	
	$R_{C-O}=1.15$	$R_{Ni-C}=1.84$	
	$k_{Ni-Ni}=0.379$[d]		

[a]From Upton and Goddard, Ref. 14.
[b]From Goddard and Allison, Ref. 20.
[c]From Richardson and Bradshaw, Ref. 21.
[d]See Ref. 13.

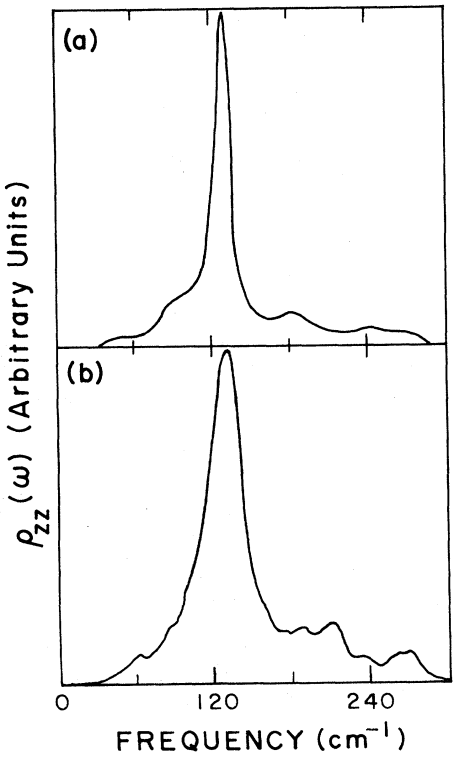

FIG. 4. We compare our calculated spectral density, for vertical motion of an atom in a clean Ni(111) surface, with the results given by Black in Ref. 21. In (a) we reproduce Black's result, and in (b) we show the results we obtain with a 76-atom cluster.

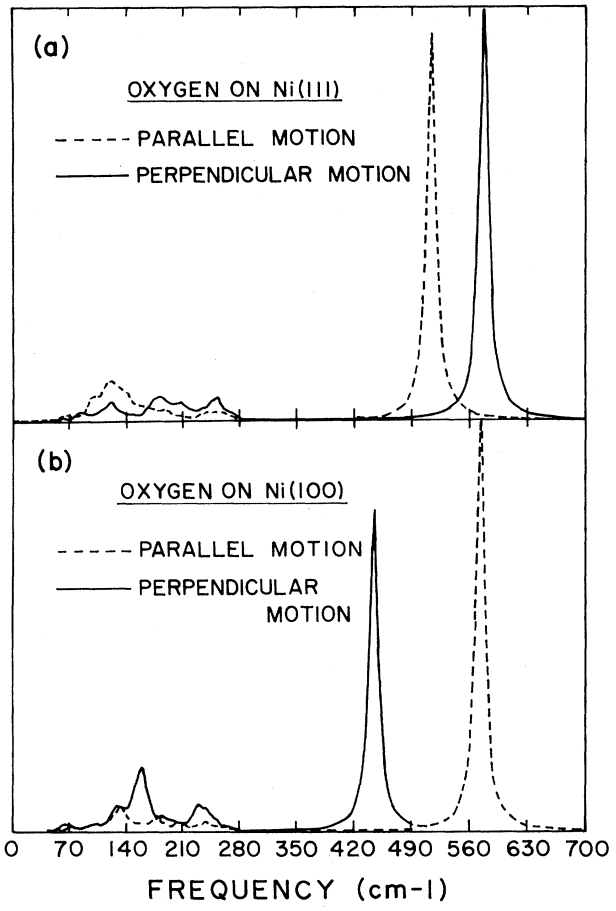

FIG. 5. We show our cluster calculations of the spectral density for parallel motion of the adsorbate (dashed lines), and for perpendicular motion (solid line), for (a) oxygen on Ni(111) and (b) oxygen on Ni(100).

bution Γ_2 to the damping rate vanishes, while the third process, Γ_3, now enters. The reverse is true for the case where oxygen resides on Ni(111), so both Γ_1 and Γ_2 are nonzero, while Γ_3 vanishes. In fact, since the adsorbate mode lies quite close to $2\omega_M$ in this case, Γ_1 is very small, and the total damping rate is dominated by Γ_2.

For the case of CO bonded linearly (top bonded) to a Ni(100)-surface atom, nearest-neighbor, bond-stretching internal coordinates alone will not adequately describe the vibrational motions. In such a model, there is zero restoring force for motion of the adsorbate parallel to the surface. In addition to coordinates which involve Ni—C or C—O stretching coordinates, one must also include restoring forces associated with coordinates in which the Ni—CO structure either deviates from linearity or is displaced away from the normal to the surface. These are angle-bending contributions to the potential energy. The first coordinate would be classified as a Ni—C—O linear bending coordinate, while the second would be referred to as a Ni—Ni—C valence angle-bending coordinate in Wilson's terminology.[19]

To ascertain the relative importance of these contributions and their influence on the spectral densities, we have made use of two different force fields from the literature. Ab initio calculations performed by Allison and Goddard[22] on a $Ni_{14}CO$ cluster provided force constants for the Ni—C and C—O stretches, as well as for the Ni—C—O bend. Alternatively, Richardson and Bradshaw[23] expanded the force field further to include not only Ni—C—O bending, but also Ni—Ni—C bending. Many of the force constants applied to their Ni_5CO cluster were deduced from gas-phase $Ni(CO)_4$ infrared data, although the Ni—C and C—O stretching force constants were fitted to the experimental results of Andersson.[24] The dependence of the linewidth of the Ni—C stretching mode on force-field selection will be discussed in Sec. IV. We now turn to a presentation of the results of our calculations of the linewidth.

IV. RESULTS AND DISCUSSION

The results of our calculations are summarized in Fig. 6, which gives the magnitude and temperature variation of the linewidth calculated for the various adsorbate/substrate combinations we have considered. While there are surely approximations at various stages of the calculation, as outlined in Secs. II and III, there are no adjustable parameters in the model. Note that we have calculated the linewidth of only the vibrational mode in which the adsorbate moves normal to the surface; it is this mode which is studied in infrared spectroscopy. As

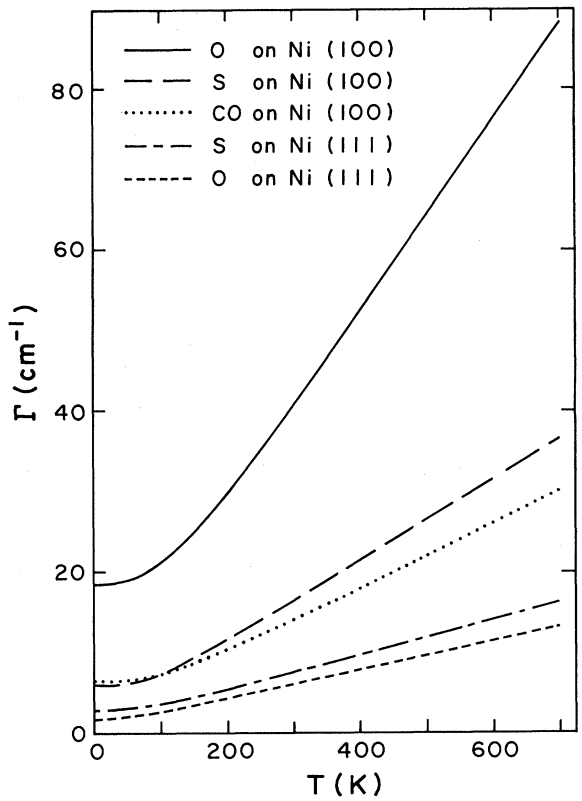

FIG. 6. Summary of the magnitude and temperature variation of our calculated linewidths for the models described in the text.

remarked in Sec. I, we have also presented a very brief discussion of these results in an earlier paper.[16] While we quoted the value of the room-temperature linewidth that we calculated for the C—Ni stretching vibration of the top-bonded CO in that discussion, we did not present its full temperature variation. Furthermore, for reasons discussed below, the linewidth for oxygen on Ni(111) was substantially underestimated, although we still find the two-phonon damping to be weak for this species. Finally, we find that Γ_3 contributes strongly to the damping of oxygen on Ni(100), and this contribution was not considered in the early version of the work.

One sees easily from Eq. (2.11) that at high temperatures, a linear temperature variation is found for the two-phonon contribution to the linewidth, while as $T \to 0$ (T denoting temperature) one obtains a residual linewidth from spontaneous two-phonon decays. The calculations show linear behavior down to roughly 100 K, a temperature well below the bulk Debye temperature (456 K) of the nickel substrate. Quite generally, high-temperature approximations to expressions such as that given in Eq. (2.11) work well down to possibly half of the Debye temperature; the elementary formula for the specific heat of a solid provided by the Debye theory shows the specific heat only falls below the high-temperature classical limit by roughly 20%, when $T = \Theta_D/2$. However, Fig. 6 shows that the linear temperature variation holds well down to a substantially lower temperature. This is a manifestation of the fact that the effective Debye temperature in the surface is substantially smaller than the bulk Debye temperature.

For oxygen and sulfur on Ni(100), the calculation shows the two-phonon contribution to the linewidth to be substantial. Our calculated value of the room-temperature linewidth for the C—Ni stretching vibration of CO, 13.9 cm^{-1}, is in excellent accord with the measured value of 15 cm^{-1},[10] as remarked previously.[23] While we are pleased with the excellent agreement between theory and experiment for this case, one must keep in mind that we have less confidence in our modeling of the anharmonicity here, when compared to the other simpler adsorbates, and also that there are approximations involved in all of the calculations. In view of this, it is particularly pleasing to see that the new values presented here for the linewidth of oxygen on Ni(100), 40 cm^{-1} at room temperature, agree well with the value inferred by Andersson, Karlsson, and Persson from their recent electron-energy-loss data for the $p(2\times2)$ oxygen overlayer on Ni(100).[17] As remarked in Sec. I, we did not consider this process in our earlier analysis. We have, incidentally, a clear explanation of why the oxygen linewidth is much larger than that for sulfur, when the two reside in the fourfold hollow site on Ni(100). That this is so was noted by Andersson and co-workers. For our model of sulfur, the parallel and perpendicular adsorbate modes lie quite close in frequency, the density of substrate modes with frequency $|\omega_0^{(\perp)} - \omega_0^{(\parallel)}|$ is thus quite small, and the calculated linewidth is dominated entirely by Γ_1. On the other hand, Γ_1 and Γ_3 both contribute to the oxygen damping rate, and both are comparable in magnitude. Our work establishes that two-phonon damping, evaluated within a realistic model, can provide linewidths comparable to those found in the data. A measurement of the temperature variation of the linewidth will play a crucial role; one must also worry about sources of inhomogeneous broadening, as discussed below, in comparing such data with theoretical curves such as those given in Fig. 6.

As remarked in Sec. III and illustrated in Table I, we have employed two different sets of force constants in our modeling of top-bonded CO. The additional angle-bending couplings are introduced because, as pointed out above, a model of top-bonded CO which contains only nearest-neighbor central force couplings provides no restoring force (in the harmonic approximation) for rigid rotations of the line that joins the Ni—C—O nuclei about the nickel-atom nucleus, or for rotation of the CO molecule about its center of mass, with the Ni held fixed. The new force constants provide the necessary restoring forces, but the new force constants influence only the low-frequency portions of the spectral density. These influence the calculated linewidths only slightly, as was noted in Sec. III when we discussed the procedure for extrapolating our cluster spectral densities from 60 cm^{-1} down to zero frequency. We find that the C—Ni stretching-mode linewidths calculated for the two models summarized in Table I agree to within a few percent.

The calculations presented here all consider an isolated adatom on an otherwise perfect single-crystal surface.

One may reasonably expect that they may also be applied to ordered overlayers where no two adsorbates bond to the same substrate atom, because then the coupling of the adsorbate to the substrate motions is dominated by the local environment.

It is quite possible that linewidth measurements may be carried out in the presence of appreciable disorder. Then it is possible that appreciable inhomogeneous broadening may occur, and this may be comparable to the intrinsic broadening which originates from anharmonicity. A pair of oxygen atoms which occupy nearest-neighbor absorption sites will have an infrared-active–mode frequency shifted somewhat from that of an isolated adsorbate. In the harmonic approximation, and in the limit of reasonably low coverage, one may suppose the infrared-absorption spectrum to be formed by simply superimposing the spectra of isolated adatoms with those of the relevant numbers of pairs, triplets, etc.

We have explored this issue within our model by calculating the frequencies of infrared-active modes of oxygen pairs on the surface, and of other small clusters of adsorbates. Consider an oxygen pair adsorbed in nearest-neighbor absorption sites on the Ni(100) surface. As long as the line between the oxygen nuclei lies in a mirror plane of the geometry, the six normal modes of the pair may be decomposed into two modes polarized normal to the mirror plane and parallel to the surface, and four modes with displacement components within the mirror plane. The former two modes are infrared inactive, and we discuss them no further. Of the remaining four modes, two lie quite close in frequency to the frequency of the isolated-oxygen parallel mode, and two are close in frequency to the isolated-oxygen perpendicular mode. All four modes are admixtures of parallel and perpendicular motion. We have explored the properties of these four modes by an analytic method discussed below and also by a cluster calculation. All modes of the pair remain polarized very nearly parallel or perpendicular to the surface, even for a nearest-neighbor pair. One of the "nearly parallel" modes becomes infrared active, i.e., the small perpendicular displacement of the two oxygens is in phase, but its oscillator strength is very small. Since its frequency is also quite close to the parallel frequency of the isolated oxygen atom, it will not contribute to the inhomogeneous broadening of the isolated adsorbate absorption line.

One of the "mostly perpendicular" modes of the pair involve coherent, in-phase, vertical motion of the oxygen pair. This mode is only slightly shifted in frequency from that of an isolated adatom, and its oscillator strength is twice that of the absorption line associated with the isolated adatom, if we assume that the dynamic dipole moment of each oxygen atom in the pair is the same as that of an isolated adatom.

The frequency shift of this mode away from the isolated adatom has been calculated by two methods: The first is an approximate analytic approach. When a light adsorbate is placed on a surface, it has been shown elsewhere[11] that one may develop a perturbation theory within which the small parameter is M_A/M_S. For both oxygen and sulfur on the Ni(100) and the Ni(111) surfaces, this method provides a quite satisfactory description of shifts induced by coupling of the adatom to the substrate motions, even though M_A/M_S is not that small. For the isolated adatom in the fourfold hollow site, with k the O—Ni force constant, this method provides the following expression for the perpendicular vibration frequency of the adatom:[3]

$$\omega_\infty^2=\frac{4k}{M_A}\left[\cos^2\alpha+\frac{M_A}{4M_s}\right], \tag{4.1}$$

where α is the angle illustrated in Fig. 1.

We have considered the two pair geometries illustrated in Table II. For the first, where the oxygen atoms each share two Ni substrate atoms, the frequency of the perpendicular infrared-active mode is

$$\omega_+^2=\frac{4k}{M_A}\left[\cos^2\alpha+\frac{M_A}{4M_s}+\frac{M_A}{8M_s}\cos^2\alpha\right], \tag{4.2}$$

while for the second geometry where the nearest-neighbor oxygens share a single Ni atom, we have

$$\omega_+^2=\frac{4k}{M_A}\left[\cos^2\alpha+\frac{M_A}{4M_s}-\frac{M_A}{16M_s}\cos(2\alpha)\right]. \tag{4.3}$$

Mode frequencies calculated from these formulas are given in Table II.

We have also calculated these frequencies by a cluster method. Through the use of clusters with 96 and 88 Ni atoms, respectively, we have calculated the frequencies of the same modes, which are also given in Table II. The two methods agree well in the first case, whereas there is a slight discrepancy in the second. The basic message is, nevertheless, very clear: The difference in frequency between the pair modes and the isolated-adatom mode lies in the range[25] 5—10 cm^{-1}. These splittings are quite comparable to the intrinsic linewidths that we have calculated. With the cluster method we have explored the frequencies of small groups of three or four oxygen atoms placed in close proximity, and have found similar shifts in the infrared-active modes.

The calculations above suggest that if intrinsic linewidth measurements are performed on surfaces where

TABLE II. Infrared-active frequencies (in cm^{-1}) for nearest-neighbor pairs of oxygen atoms placed on the Ni(100) surface. Two configurations are considered. For the case where the oxygen pair shares a bond with one Ni atom, 96 Ni atoms are used in the basic cluster, while for the case where the two oxygens share two Ni atoms, 88 Ni atoms are used. (The isolated-oxygen-atom frequency is 445 cm^{-1}).

	Theory	Cluster calculation
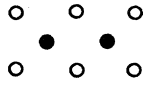	450.9[a]	449.4
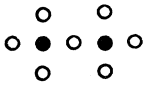	439.0[b]	433.0

[a]Equation (4.2).
[b]Equation (4.3).

there is appreciable disorder in the adsorbates, then inhomogeneous broadening with an origin in clustering of the adsorbates may be comparable to that provided by anharmonic damping. This may partially mask the strong temperature dependence displayed in Fig. 6. We plan further, more complete studies of inhomogeneous broadening produced by disorder. These will be reported elsewhere.

ACKNOWLEDGMENTS

The research of two of us (J.C.A. and D.L.M.) was supported by the U.S. Department of Energy through Contract No. DE-AT0379-ER10432. The research of the other two of us (K.G.L. and J.C.H.) was supported by the Office of Naval Research (U.S. Department of the Navy).

[1]For a review of early work in the field, see R. F. Wallis, Prog. Surf. Sci. **4**, 233 (1973).

[2]H. Ibach and D. L. Mills, *Electron Energy Loss Spectroscopy and Surface Vibrations,* (Academic, San Francisco, 1982).

[3]G. Borusdeylins, R. B. Doak, and J. P. Toennis, Phys. Rev. Lett. **46**, 437 (1981); Phys. Rev. B **27**, 366 (1983); R. B. Doak, U. Harten, and J. P. Toennis, Phys. Rev. Lett. **51**, 578 (1983).

[4]S. Lehwald, J. Szeftel, H. Ibach, T. S. Rahman, and D. L. Mills, Phys. Rev. Lett. **50**, 518 (1983); J. Szeftel, S. Lehwald, H. Ibach, T. S. Rahman, J. E. Black, and D. L. Mills, *ibid.* **51**, 268 (1983).

[5]See R. Ryberg, Surf. Sci. **114**, 627 (1982).

[6]Y. Chabal and A. J. Sievers, Phys. Rev. Lett. **44**, 944 (1980).

[7]Y. Chabal, Phys. Rev. Lett. **50**, 1850 (1983).

[8]D. L. Mills, C. J. Duthler, and M. Sparks, in *Disordered Solids, Optical Properties,* Vol. 4 of *Dynamical Properties of Solids,* edited by G. K. Horten and A. A. Maradudin (North-Holland, Amsterdam, 1980).

[9]A number of references to theoretical studies of the damping of adsorbate vibrations by particle-hole pairs may be found in Ref. 3. See, most particularly, B. N. J. Persson and M. Persson, Surf. Sci. **97**, 609 (1980); M. A. Kozhushner, V. G. Kustarev, and B. R. Shub, *ibid.* **81**, 261 (1979).

[10]S. Chiang, R. G. Tobin, and P. L. Richards, Bull. Am. Phys. Soc. **28**, 503 (1982); S. Chiang, R. Tobin, P. L. Richards, and P. A. Thiel, Phys. Rev. Lett. **52**, 648 (1984).

[11]See the discussion in *Electron Energy Loss Spectroscopy and Surface Vibrations,* Ref. 2, Chap. 4.

[12]Horia Metiu and Willam E. Palke, J. Chem. Phys. **69**, 2574 (1978).

[13]The model described is that discussed in Ref. 11; it has also been applied to a variety of discussions of the coupling of adsorbate vibrations to substrate motions. For examples, see T. S. Rahman, J. E. Black, and D. L. Mills, Phys. Rev. B **25**, 883 (1982); **27**, 4059 (1983); J. E. Black, Talet S. Rahman, and D. L. Mills, *ibid.* **27**, 4072 (1983); J. M. Szeftel, S. Lehwald, H. Ibach, T. S. Rahman, J. E. Black, and D. L. Mills, Phys. Rev. Lett. **51**, 268 (1983). Recently, Andersson, Karlsson, and Persson have employed this model, with the same scheme for choosing parameters discussed in the references just cited, to reproduce a number of our earlier results. [See S. Andersson, P. A. Karlsson, and M. Persson, Phys. Rev. Lett. **51**, 2378 (1983)].

[14]Thomas H. Upton and W. A. Goddard III, Phys. Rev. Lett. **46**, 1635 (1981).

[15]J. E. Black, B. Laks, and D. L. Mills, Phys. Rev. B **22**, 1818 (1980).

[16]J. C. Ariyasu, D. L. Mills, Karthryn, G. Lloyd, and John C. Hemminger, Phys. Rev. B **28**, 6123 (1983).

[17]S. Andersson, P. A. Karlsson, and M. Persson, Phys. Rev. Lett. **51**, 2378 (1983).

[18]See the discussion in *Electron Energy Loss Spectroscopy and Surface Vibrations,* Ref. 2, Chap. 5.

[19]See E. B. Wilson, Jr., J. C. Decius, and P. C. Cross, *Molecular Vibrations* (McGraw-Hill, New York, 1955).

[20]D. Steele, *Theory of Vibrational Spectroscopy* (W. B. Saunders, Philadelphia, 1971).

[21]J. E. Black, Surf. Sci. **105**, 59 (1981).

[22]J. N. Allison and W. A. Goddard III, Surf. Sci. **115**, 553 (1982).

[23]N. V. Richardson and A. M. Bradshaw, Surf. Sci. **88**, 255 (1979).

[24]S. Anderson, Solid State Commun. **21**, 75 (1977); *Proceedings of the Seventh International Vacuum Congress and the Third International Conference on Solid Surfaces* (R. Dombrozemsky *et al.*, Vienna, 1977), p. 815.

[25]In our model such splittings are found for pairs and small clusters within which a given Ni atom bonds to more than one oxygen. In less dense clusters, where oxygens are in close proximity but any Ni substrate atom is bonded to one and only one oxygen, the shifts are much smaller. One may appreciate this from the structure of the perturbation theory used to generate Eqs. (4.2) and (4.3).